The soluble epoxide hydrolase encoded by EPXH2 is a bifunctional enzyme with novel lipid phosphate phosphatase activity

John W. Newman*, Christophe Morisseau*, Todd R. Harris, and Bruce D. Hammock†

Department of Entomology and University of California Davis Cancer Center, University of California, One Shields Avenue, Davis, CA 95616

Contributed by Bruce D. Hammock, December 18, 2002

The gene *EPXH2* encodes for the soluble epoxide hydrolase (sEH), an enzyme involved in the regulation of cardiovascular and renal physiology containing two distinct domains connected via a proline-rich linker. The C-terminal domain containing the EH catalytic activity has been well studied. In contrast, a function for the N-terminal domain, which has high homology to the haloacid dehalogenase family of phosphatases, has not been definitively reported. In this study we describe the N-terminal domain as a functional phosphatase unaffected by a number of classic phosphatase inhibitors. Assuming a functional association between these catalytic activities, dihydroxy lipid phosphates were rationalized as potential endogenous substrates. A series of phosphorylated hydroxy lipids were therefore synthesized and found to be excellent substrates for the human sEH. The best substrate tested was the monophosphate of dihydroxy stearic acid (*threo*-9/10-phosphonoxy-hydroxy-octadecanoic acid) with $K_m = 21 \pm 0.3$ μM, $V_{Max} = 338 \pm 12$ nmol·min^{-1}·mg^{-1}, and $k_{cat} = 0.35 \pm 0.01$ s^{-1}. Therefore dihydroxy lipid phosphates are possible candidates for the endogenous substrates of the sEH N-terminal domain, which would represent a novel branch of fatty acid metabolism with potential signaling functions.

The soluble epoxide hydrolase (sEH), first described in 1972 (1), is an ubiquitous enzyme in vertebrates that transforms epoxides to their corresponding diols (2). Although uniformly expressed in the liver, high expression of sEH is highly localized in other tissues including vascular endothelium, some smooth muscle, and the proximal tubule (3, 4). Epoxy fatty acids generated by cytochrome P450 epoxygenases are endogenous substrates for the sEH C-terminal domain (5), with critical roles in the regulation of cardiovascular, renal, and inflammatory biology (6–9). The hydrolysis of epoxy fatty acids modulates their intracellular fate (10, 11) and biological activity (9, 12, 13). *In vivo*, the pharmacological blockade of epoxide hydrolysis attenuates hypertension (4, 14), whereas the deletion of this gene reduces blood pressure in male mice to female levels (15).

The sEH is a homodimer with a monomeric unit of 62.5 kDa (2) whose primary structure suggests that the *EPXH2* gene was produced by the fusion of two primordial dehalogenase genes (16, 17). This gene fusion hypothesis was recently supported by a 2.8-Å resolution x-ray crystal structure of the mouse enzyme (18). The C-terminal sEH domain has high homology to haloalkane dehalogenase, whereas the N-terminal domain is similar to haloacid dehalogenase (HAD). Although analysis of the sEH crystal structure revealed that the conserved HAD-like catalytic residues were properly oriented for catalysis, no dehalogenase activity was detected (18). However, the amino-terminal catalytic DXDX(T/V) motif of HAD has been used to describe an enzyme class that includes numerous phosphatases (19–21).

It can be argued that gene fusion events are driven by evolution, leading to the physical linkage of functionally associated proteins (22, 23). Therefore, we hypothesized that endogenous products of sEH metabolism (i.e., dihydroxy fatty acids) may be enzymaticly phosphorylated *in vivo* to produce substrates for the sEH N-terminal domain. This article describes the evaluation of hydroxy lipid phosphates as substrates for the sEH N-terminal catalytic site, while performing a biochemical characterization of this activity.

Materials and Methods

Reagents. The 12-hydroxy stearic acid, ricinelaidic acid, and ricinoleic acid were purchased from NuChek Prep (Elysian, MN). Dihydroxy fatty acids were synthesized as described (12, 24). HPLC grade chloroform ($CHCl_3$), triethylamine (TEA), and glacial acetic acid were purchased from Fisher Scientific. OmniSolv acetonitrile and methanol (MeOH) were purchased from EM Science. Other reagents were purchased from either Sigma or Aldrich Chemical (Milwaukee, WI), unless otherwise indicated.

Enzyme Preparations. Recombinant human sEH (HsEH) was produced in a baculovirus expression system (16) and purified by affinity chromatography (25) in Tris·HCl buffer (100 mM, pH 7.4). The preparations were at least 97% pure as judged by SDS/PAGE and scanning densitometry. No detectable esterase or glutathione transferase activities were observed. Recombinant forms of WT and mutant (Y465F) mouse sEH (MsEH), human microsomal EH (mEH), and mouse-eared cress sEH were produced in a baculovirus expression system as described (26–28). A 10,000-g supernatant was used for the measurement and comparison of enzyme activities. Western blot analyses indicated equivalent protein expression for each system. Protein concentrations were quantified with the Pierce BCA assay using BSA as the calibrating standard. The EH activity was measured by using 50 μM substrate: racemic [^{3}H]*trans*-1,3-diphenylpropene oxide for sEH (29) and [^{3}H]*cis*-stilbene oxide for mEH (30).

Lipid Phosphate Synthesis. The *in situ* generation of an activated phosphoimidate was used to phosphorylate hydroxy fatty acids (31). Briefly, 100 mg of hydroxy lipid was dissolved in 0.8 ml of 1:1 acetonitrile/DMSO (vol/vol) and enriched with 150 μl of TEA, followed by 60 μl of trichloroacetonitrile and 40 μl of 85% phosphoric acid. The mixture was stirred at 50°C for 30 min. The acetonitrile was then evaporated, and the resulting residue was extracted with 2 ml of 2:1:1 $CHCl_3$/MeOH/water (vol/vol/vol). The aqueous phase was reduced to dryness under vacuum, redissolved in 10 ml of 5% methanol in water, and extracted by using 1-g C18 solid-phase extraction (SPE) cartridges (Varian). Phosphorylated products were eluted from the column with <40% MeOH in water. Collected fractions were extracted with 100 mg of strong anion-exchange SPE cartridges (Agilent Technologies, Wilmington, DE), and lipid phosphates were eluted with a step gradient of 0–1% TEA in MeOH. Fractions were

Abbreviations: EH, epoxide hydrolase; sEH, soluble EH; HsEH, human sEH; MsEH, mouse sEH; mEH, microsomal EH; TEA, triethylamine; ESI, electrospray ionization; LC, liquid chromatography; CV, collision voltage; PHO, phosphonoxy-hydroxy octadecanoic acid; *para*-NPP, *para*-nitrophenyl phosphate; AP_{HP}, human placental alkaline phosphatase.

*J.W.N. and C.M. contributed equally to this work.

†To whom correspondence should be addressed. E-mail: bdhammock@ucdavis.edu.

www.pnas.org/cgi/doi/10.1073/pnas.0437724100

Table 1. Hydroxy lipid phosphate characterization

Compound	Structure	Yield, %	Mass, $[M-H]^-$	^{31}P-NMR, ppm
12-Phosphonooxy-octadecanoic acid (12-PO)	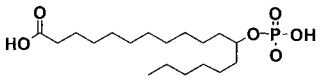	3.8	379.2377 (379.2328)	1.5
12-Phosphonooxy-octadec-9*E*-enoic acid (12-PO(9*E*)ME)	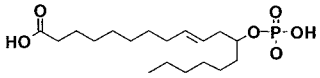	10	377.2154 (377.2171)	2.1
12-Phosphonooxy-octadec-9*Z*-enoic acid (12-PO(9*Z*)ME)	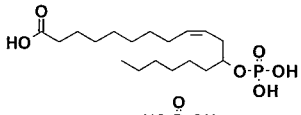	13	377.2184 (377.2171)	1.4
erythro-9,10-phosphonooxy-hydroxy-octadecanoic acid (*erythro*-9/10-PHO)	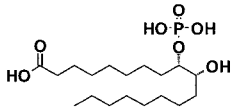	4.4	395.2238 (395.2277)	1.1
threo-9,10-phosphonooxy-hydroxy-octadecanoic acid (*threo*-9/10-PHO)	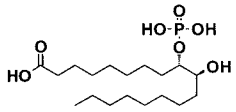	1.1	395.2176 (395.2277)	1.0

Analyte purity was >90% except for *erythro*-PHO (≈85% pure). Although a single structure is shown, diol phosphates are 1:1 mixtures of the monophosphate of each possible alcohol. Measured anionic masses are shown with theoretical masses in parentheses.

screened for purity by electrospray ionization (ESI)-liquid chromatography (LC)/MS and solvent was removed under vacuum. For diol monophosphate isolation, lyophilization was required to prevent degradation. Fractions containing pure monophosphates were combined and evaluated by ^{1}H- and ^{31}P-NMR in deuterated methanol relative to a phosphoric acid external standard by using a Mercury 300 NMR (Varian). High-resolution mass spectra were acquired on a time-of-flight mass spectrometer (Micromass, Manchester, U.K.) by using negative-mode ESI and leucine enkephalin as a lock mass compound. Lipid phosphates were uniformly isolated in low yield as 1:1 TEA salts (Table 1). Diol monophosphates were 1:1 regioisomeric mixtures. Analyte-to-amine ratios were quantified from ^{1}H-NMR spectra. Chemical purity was estimated at >90% for each compound based on ^{1}H-NMR spectra, the presence of a single phosphorus species, and ESI-LC/MS analyses. Negative-mode ESI showed a single peak, whereas positive mode confirmed TEA as the only ESI-LC/MS-detectable secondary component, unless otherwise indicated.

Tandem Quadrupole MS. The quantification of all lipids was performed by using HPLC with ESI and tandem mass spectrometric detection (MS/MS). A Waters 2790 separation module was directly interfaced with the ESI probe of a Quattro Ultima tandem-quadrupole mass spectrometer (Micromass). A cone gas flow of 125 liter/h, desolvation gas flow of 650 liters/h, source temperature of 125°C, desolvation temperature of 400°C, ESI capillary voltage of −3.0 kV, and ESI cone voltage of 50 V were used for all analyses. For MS/MS experiments, argon was used as the collision gas at a pressure of 2.3×10^{-3} Torr, and quadrupole mass resolution settings were fixed at 12.0 (i.e., ≈1.5-Da resolution). The photo multiplier voltage was 650 V. Optimal collision voltages (CVs) were established experimentally, and ion dwell times of 0.40 s were used.

Phosphate Hydrolysis. Assays for hydroxy lipid phosphate hydrolysis were performed by using a 2.0 × 20 mm, 3-μm Luna C18(2) Mercury MS column (Phenomenex, Torrance, CA) with a 350 μl/min isocratic flow of 61:28:11 (vol/vol/vol) acetonitrile/water/MeOH with 0.1% glacial acetic acid for 2.5 min. Released hydroxy lipids were detected at the retention time (t_R) of external standards in multireaction monitoring mode by using optimized CV for characteristic mass transitions (m/z precursor ion > product ion): *erythro*- and *threo*-dihydroxy stearate (t_R = 0.7 and 0.8 min, CV = 15 V, m/z 315.2 > 297.2); ricinelaidate and ricinoleate (t_R = 1.0 and 1.1 min, CV = 15 V, m/z 299.2 > 183.0); hydroxy stearate (t_R = 1.2 min, CV = 26 V, m/z 299.2 > 281.2). Lipids were quantified relative to an internal standard, 10,11-dihydroxy nonadecanoic acid (t_R = 0.9 min, CV = 26 V, m/z 329.2 > 311.2). The hydrolysis of other phosphates was measured by the spectrophotometric detection of either *para*-nitrophenol (ε_{405} = 18,530 $M^{-1}\cdot cm^{-1}$) or the released inorganic phosphate as a molybdenum salt (ε_{623} = 99,600 $M^{-1}\cdot cm^{-1}$) as reported (21).

Phosphatase Assay Optimization. All enzyme reactions were run in triplicate along with appropriate buffer and enzyme controls, and differences between means were evaluated by using a Student's *t* test. A crude mixture (≈85% pure) of *erythro*-9/10-phosphonoxy-hydroxy octadecanoic acid (*erythro*-PHO) was used as the substrate for assay optimization. This mixture was contaminated with ≈5% diol and 10% of the 9,10-cyclic phosphate. Under the assay conditions, the cyclic phosphate was not hydrolyzed. Reactions were run at 100 μl, halted with the addition of 0.4 ml of methanol, spiked with internal standard (≈1 pmol), and analyzed by LC/MS/MS as described above. Assay conditions were varied to maximize phosphatase activity, while containing substrate hydrolysis to <5%. Magnesium-dependent phosphatase activity was confirmed in initial incubations of recombinant HsEH with 50 μM *erythro*-PHO (vehicle = 1 μl ethanol) performed in the presence of either 1 mM sodium EDTA or 1 mM $MgCl_2$ under standard sEH assay conditions (100 mM sodium phosphate at pH 7.4 with 0.1 mg/ml BSA, for 10 min at 30°C).

The effect of buffer salts and pH on phosphatase activity was evaluated at 0.5 pH unit intervals in 0.1 M solutions of sodium phosphate (pH 6.0–7.5), Tris·HCl (pH 6.5–9.0), and Bis Tris·HCl (pH 5.5–7.5). Maximal phosphatase-specific activity (10× ini-

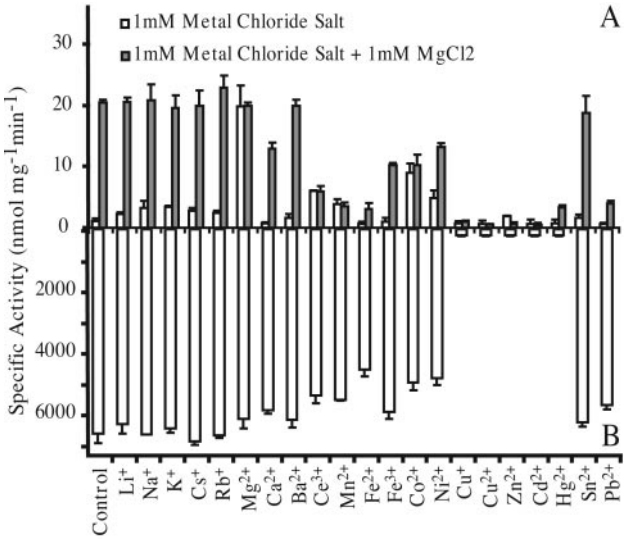

Fig. 1. Effect of cation chloride salts on the sEH-catalyzed hydrolysis of *erythro*-9,10-PHO (*A*) and *trans*-1,3-diphenyl propene oxide (*B*). Reactions were conducted with affinity-purified HsEH as described in the text. Results are the mean ± standard deviation of triplicate analyses.

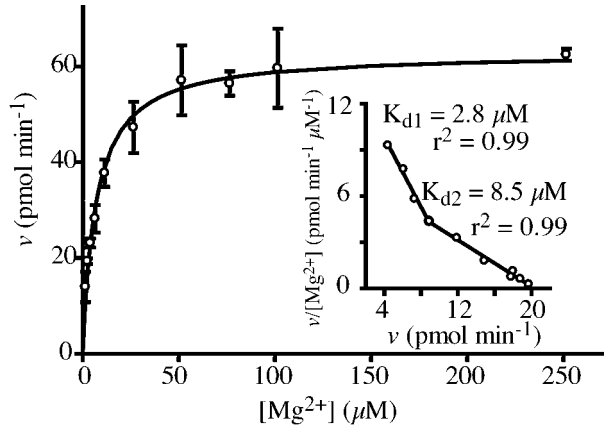

Fig. 2. The magnesium ion dissociation constants were determined by the kinetic analysis of Mg^{2+}-dependent *erythro*-9,10-PHO hydrolysis. Substrate (50 μM) was incubated in triplicate with affinity-purified HsEH in the presence of between 1 μM and 5 mM $MgCl_2$, in three separate experiments. Shown is the mean ± standard deviation of one analysis documenting activity saturation at ≈100 μM $MgCl_2$. Corrections for background activity were performed as described in the text. Compiling the results revealed two Mg^{2+} dissociation constants (K_{d1} = 4.0 ± 1.0 μM and K_{d2} = 7.8 ± 1.3 μM) as shown in the Scatchard plot (*Inset*).

tial) was observed in Bis Tris·HCl at pH 7.0. The effect of buffer osmolarity was then evaluated with 10, 25, 50, and 100 mM Bis Tris·HCl (pH 7.0), with 25 mM showing maximal activity (data not shown). Incubating 11.5 μg/ml (≈180 nM) HsEH with 50 μM *erythro*-PHO in 25 mM Bis Tris·HCl (pH 7.0) with 1 mM $MgCl_2$ at 30°C showed a linear rate of diol formation in pmol·min^{-1} ($y = 12.0\times + 15.6$; $r^2 = 0.993$) for up to 30 min. Increasing the enzyme concentration in 5-min incubations elevated activity in a linear fashion between 5 and 23 μg/ml (r^2 = 1.00). Up to 0.2 mg/ml BSA did not influence phosphate hydrolysis.

Therefore, sEHs (11.5 μg/ml) were incubated with 50 μM of substrate for 10 min at 30°C in Bis Tris·HCl (25 mM, pH 7.0) containing 0.1 mg/ml BSA and 1.0 mM $MgCl_2$, unless otherwise indicated. The human placental alkaline phosphatase (AP_{HP}) activity was measured in Tris·HCl buffer (100 mM, pH 9.0) with 1 mM $MgCl_2$, 0.1 mM $ZnCl_2$, and 0.1 mg/ml BSA at 30°C.

Inhibition Experiments. EH and phosphatase activity was assessed as described above after a 5-min preincubation with inhibitors. For sEH activity, 50 μM of either *trans*-diphenyl propene oxide or *erythro*-PHO were used to assess EH and phosphatase activity, respectively. The activity of AP_{HP} was evaluated by using 5 mM *para*-nitrophenyl phosphate (*para*-NPP), providing a phosphatase inhibition control.

Kinetic Assay Conditions. Purified HsEH was incubated with *para*-NPP ($0.25 < [S]_{final} < 10.0$ mM) and *threo*-9/10-PHO ($1.0 < [S]_{final} < 100.0$ μM) at 30°C. Velocity of phosphate hydrolysis was measured as described under assay conditions. Kinetic constants were determined for both *para*-NPP and *threo*-PHO following the method described by Hill for allosteric enzymes (32). Plots of reaction velocity (v) as a function of substrate concentration ([S]) allow the determination of apparent kinetic constants. Resolution of the nonlinear Hill equation, i.e., $v = (V_{Max}[S]^n)/(K + [S]^n)$, was performed by using SIGMA PLOT (SPSS, Chicago). The concentration of substrate for which half of the maximum velocity was obtained, i.e., K_m, was calculated by using the following equation: $K_m = (K)^{1/n}$. The Hill coefficient (n) was determined from the Hill plot: $\ln(v/V_{Max} - v)$ vs. $\ln([S])$, where n is the slope of the obtained line. The results are presented as mean ± the standard deviation of three separate determinations of K_m, V_{Max} , and n.

Results

Cation Effect on Phosphatase and EH Activity. To evaluate the effect of cations on both dihydroxy lipid phosphate and epoxide hydrolysis, reactions were conducted with a series of cation chloride salts at concentrations of 1 mM (Fig. 1). The metallic oxidants, copper, zinc, cadmium, and mercury inhibited both catalytic activities. The phosphatase activity was maximally enhanced by magnesium, whereas cobalt produced ≈50% of the Mg^{2+}-dependent activation. Reactions were then repeated for each of the cation chloride salt (1 mM) with the addition of $MgCl_2$ (1 mM) to assess the cation series for inhibitors of the Mg^{2+}-dependent phosphatase activity. Many of the divalent cations inhibited the Mg^{2+}-dependent activity to varying degrees.

Mg^{2+} Dissociation Constants. The magnesium ion dissociation constants were determined by the kinetic analysis of magnesium-dependent *erythro*-PHO hydrolysis. Reactions were conducted at $MgCl_2$ concentrations between 1 μM and 5 mM. Replacing $MgCl_2$ with $MgSO_4$ produced indistinguishable results (data not shown). Analysis of the Michaelis–Menten plot of velocity vs. Mg^{2+} concentration indicated 1.5-μM magnesium equivalents were present in the absence of magnesium additions. The background activation could be eliminated by incubation with EDTA, but not by enzyme pretreatment with the chelator during the purification process, suggesting trace impurities in the assay reagents. The 1.5-μM value was used to adjust apparent Mg^{2+} concentrations before dissociation constant determinations. Fig. 2 shows the mean ± standard deviation of one of three independent analyses. Two Mg^{2+} dissociation constants were detected ($K_{d1} = 4.0 \pm 1$ μM and $K_{d2} = 7.8 \pm 1$ μM). A Hill coefficient of 1.0 ± 0.2 was calculated, suggesting a single Mg^{2+} ion is associated per catalytic subunit.

N-Terminal Domain Dependence. A series of baculovirus-expressed enzymes were assayed for *erythro*-PHO hydrolysis to evaluate the dependence of the observed phosphatase activity on the N-terminal domain (Table 2). The hydrolysis of epoxide-containing surrogate substrates showed that all of the tested enzymes had measurable

Table 2. Catalytic activity of several epoxide hydrolases

Enzymes	Specific activity, nmol·min^{-1}·mg^{-1}	
	Epoxide hydrolysis	Phosphate hydrolysis
Affinity purified		
HsEH	5,831 ± 367	95.4 ± 6.0
10,000 g Supernatants		
HsEH	1,115 ± 86	38.7 ± 2.2
MsEH	2,825 ± 87	58.3 ± 7.3
MsEH Y465F	15.4 ± 0.2	13.6 ± 1.0
Cress sEH	453 ± 39	<0.3*
Human mEH	6.4 ± 0.2	<0.3

*Detection limit = three times background.

EH activity. The mammalian sEHs, including a sEH catalytic site mutant (MsEH Y465F), showed measurable phosphatase activity. However, the C-terminal domain mutant showed an ≈5-fold decrease in phosphatase activity. Previous studies suggest this change is not caused by altered folding in the mutant (26). Conversely phosphatase activity was not detected in either the plant sEH or human mEH. The cress sEH is homologous to the mammalian sEH C-terminal domain (28), whereas the sEH and mEH N-terminal domains are not homologous (17).

sEH and Phosphatase Inhibitors. To assess the potential for communication between the EH and phosphatase domains, these two catalytic activities were assessed in the presence of various inhibitors (Table 3). First, two classes of potent sEH inhibitors were evaluated. Chalcone oxides are epoxide-containing competitive substrates with high nM to low μM K_is (33), whereas di-substituted ureas are stable transition-state mimics of the C-terminal catalytic site with low nM K_is (34–36). A maximum phosphatase inhibition of 10% was observed for the sEH inhibitors tested. Finally, the enzyme was challenged with a series of phosphatase inhibitors (21, 37) by using AP_{HP} as a positive control: activated orthovanadate (general phosphate-transferase inhibitor), fluoride (ATPase inhibitor), tartrate and molybdate (acid phosphatase inhibitors), and okadaic acid (Ser/Thr protein phosphatase inhibitor). The only phosphatase inhibition observed was by sodium orthovanadate acting on AP_{HP}.

Substrate Specificity. The preceding experiments demonstrated that dihydroxy lipid phosphates are substrates for the sEH N-terminal domain. Subsequent experiments were conducted to evaluate: (*i*) the specificity of the sEH phosphatase activity for hydroxy lipid phosphates and (*ii*) the ability of a promiscuous phosphatase to metabolize these compounds. To address the first issue, a series of hydroxy lipid phosphates was synthesized and assessed as substrates of the purified HsEH along with a series of commercially available phosphates. For the second issue, the same phosphate series was assessed as substrates of AP_{HP}. The resulting specific activities are shown in Table 4. Dihydroxy lipid phosphates were found to be the best substrates for the HsEH, with the *threo*-isomer being hydrolyzed approximately three times faster than the *erythro*-form. Monohydroxy lipid phosphates were also hydrolyzed by this enzyme at a lower rate. Finally, the addition of a double bond enhanced the rate of substrate hydrolysis with the cis-olefinic species being hydrolyzed approximately five times faster than the trans form.

In addition to the substrates shown, neither enzyme showed phosphatase activity with 5 mM of di-*para*-NPP, phytic acid, *O*-phospho-L-serine, *O*-phospho-L-tyrosine, or phosphatidic acid. Of the commercial phosphates tested, only *para*-NPP was hydrolyzed by HsEH at a significant rate. Many of the commercial phosphates, as well as the hydroxy lipid phosphates, were hydrolyzed by AP_{HP}, indicating that the assays themselves performed well. As opposed to the HsEH lipid phosphate metabolism, the addition and configuration of double bonds had only a minimal effect on AP_{HP} metabolism. Also, in the case of *erythro*-PHO, increasing the substrate concentration 10-fold enhanced AP_{HP}-dependent hydrolysis six times, suggesting a K_m in the mM range for AP_{HP} and this substrate.

Enzyme Kinetics. Enzyme kinetic measurements were performed for the HsEH-dependent metabolism of *para*-NPP and *threo*-PHO, allowing a comparison of the enzymes' catalytic efficiency for these two substrates. The dihydroxy lipid phosphate had both a lower K_m and higher V_{Max} than that of *para*-NPP (Table 5). Comparing the k_{cat}/K_m ratio for these two substrates indicates that the sEH metabolizes *threo*-PHO more efficiently than *para*-NPP. In addition, only the *threo*-PHO showed positive cooperativity (Hill coefficient = 1.9; Fig. 3).

Discussion

The results of the present study clearly show that both MsEHs and HsEHs are magnesium-dependent phosphatases. Evaluations of a plant sEH, which contains only the C-terminal domain,

Table 3. Effect of inhibitors on EH and phosphatase activity

Effectors	Concentration, mM	Inhibition, %		
		^{EH}HsEH	^{Phos}HsEH	AP_{HP}
Vehicle control	—	0 ± 3	0 ± 7	0 ± 10
Epoxide hydrolase inhibitors				
Chalcone oxide	0.1	80 ± 1*	0 ± 10	0 ± 10
4-Fluoro-chalcone oxide	0.1	87 ± 2*	8 ± 4	0 ± 8
4-Phenyl-chalcone oxide	0.1	100 ± 1*	11 ± 1*	0 ± 3
1-Cyclohexyl-3-ethyl urea	0.1	54 ± 3*	0 ± 10	3 ± 13
1-Cyclohexyl-3-hexyl urea	0.1	100 ± 1*	4 ± 5	0 ± 14
1,3-Dicyclohexyl urea	0.1	100 ± 1*	0 ± 4	6 ± 13
1-Cyclohexyl-3-dodecyl urea	0.1	100 ± 1*	0 ± 3	0 ± 9
Phosphatase inhibitors				
Okadaic acid	0.1	12 ± 3*	3 ± 8	0 ± 7
Tartaric acid	1.0	2 ± 3	2 ± 1	0 ± 14
Sodium fluoride	1.0	1 ± 7	10 ± 4	12 ± 8
Sodium orthovanadate	1.0	9 ± 7	0 ± 5	82 ± 13*
Sodium molybdate	1.0	0 ± 1	8 ± 2	0 ± 5

^{EH}HsEH: HsEH EH activity; ^{Phos}HsEH: HsEH phosphatase activity.
*Significant inhibition relative to vehicle control ($P < 0.05$).

BIOCHEMISTRY

Table 4. Comparison of sEH and alkaline phosphatase substrate specificities

Substrates	Concentration, mM	Specific activity, nmol·min^{-1}·mg^{-1} HsEH	Specific activity, nmol·min^{-1}·mg^{-1} AP_{HP}
threo-9/10-PHO	0.05	324 ± 20	829 ± 29
erythro-9/10-PHO	0.05	95.4 ± 6.0	554 ± 2
erythro-9/10-PHO	0.5	104 ± 7.5	3,050 ± 95
12-PO(9*Z*)ME	0.05	117 ± 18	379 ± 15
12-PO(9*E*)ME	0.05	20.9 ± 1.0	370 ± 20
12-PO	0.05	9.9 ± 2.7	365 ± 89
para-NPP	5.0	35.6 ± 2.0	2,540 ± 71
Glucose-6-phosphate	5.0	9.4 ± 2.9	36.0 ± 1.2
Creatinine phosphate	5.0	0.6 ± 1.2	11.6 ± 2.3
Adenosine triphosphate	5.0	1.4 ± 6.1	17.3 ± 0.3
α-Glycerophosphate	5.0	4.0 ± 1.6	45.5 ± 0.1
β-Glycerophosphate	5.0	7.3 ± 9.2	37.8 ± 0.4

See Table 1 for complete names of substrates.

clearly link the phosphatase activity to the N-terminal domain. The effect of classic sEH inhibitors suggested that the two catalytic sites are functionally distinct. However, the decrease in the specific activity of the C-terminal domain catalytic site mutant would seem to indicate some degree of communication between these two sites. Assessment of the magnesium binding kinetics revealed two distinct Mg^{2+} dissociation constants of ≈4 and 8 μM, respectively. Because the sEH forms a functional homodimer (2), the two Mg^{2+} binding sites likely represent each of the two N-terminal catalytic sites in the dimeric complex and cooperativity may exist between these two sites effecting the relative binding affinity of the cofactor. Interestingly, phosphatase inhibitors reported to effect other DXDX(T/V) type phosphatases, i.e., sodium orthovanadate, (21) failed to block the sEH phosphatase activity, as did all other tested phosphatase inhibitors. In addition, while the sEH was able to hydrolyze *para*-NPP, the K_m for this substrate was >1 mM, and other tested commercially available phosphates were not hydrolyzed. Together, these results suggest that the sEH–phosphatase domain has high specificity for lipophilic phosphates.

Assuming a functional association between the substrates of the two sEH catalytic domains led to the hypothesis that the N-terminal domain would efficiently metabolize dihydroxy lipid monophosphates. When tested the hydroxy lipid phosphates were in fact found to be excellent substrates for this enzyme. Inspecting a short series of 12-hydroxy octadecanoids, it was found that the addition of a single double bond β to the phosphonoxy group increased the rate of substrate turnover relative to the saturated compound. In addition, if the olefin had a cis configuration, the rate of hydrolysis was ≈5-fold greater than the trans isomer. Moreover, the phosphate of a *threo*-diol, which results from the enzymatic hydrolysis of a *cis*-epoxide, was hydrolyzed ≈3-fold faster than the corresponding *erythro*-diol. In fact, *threo*-PHO was the best substrate (K_m = 20 μM) identified within the limited series tested. Comparing the k_{cat}/K_m ratio of the *threo*-PHO with that of *para*-NPP indicated that the enzyme was ≈450-fold more specific for the lipid phosphate. In addition, these high-affinity substrates revealed positive cooperativity not observed with *para*-NPP, suggesting concentration and/or substrate-dependent allosteric interactions within the protein. The use of a 1:1 isomeric mixture of dihydroxy monophosphates could present complicated kinetics if both isomers compete for the active site with different affinities. However, because substrate hydrolysis was maintained at <5% during incubations, the kinetics should be dominated by the high-affinity substrate.

Table 5. Kinetic constants for HsEH substrate hydrolysis

Kinetic parameters	*threo*-PHO	*para*-NPP
K_m, μM	20.9 ± 0.30	1,600 ± 140
V_{Max}, nmol·min^{-1}·mg^{-1}	338 ± 12	57.6 ± 2.5
k_{cat}, s^{-1}	0.35 ± 0.01	0.060 ± 0.003
k_{cat}/K_m, M^{-1}·s^{-1}	16,700 ± 22	43.4 ± 0.47
Hill coefficient	1.9 ± 0.1	1.0 ± 0.0

Therefore, with the identification of the sEH as a functional phosphatase with high affinity for hydroxy, and particularly *threo*-dihydroxy lipid phosphates, a picture emerges suggesting the existence of a novel branch of fatty acid metabolism emanating from the P450-dependent oxidation of unsaturated lipids (Fig. 4). The positive influence of cis double bonds on substrate hydrolysis further supports this idea. Comparing the catalytic

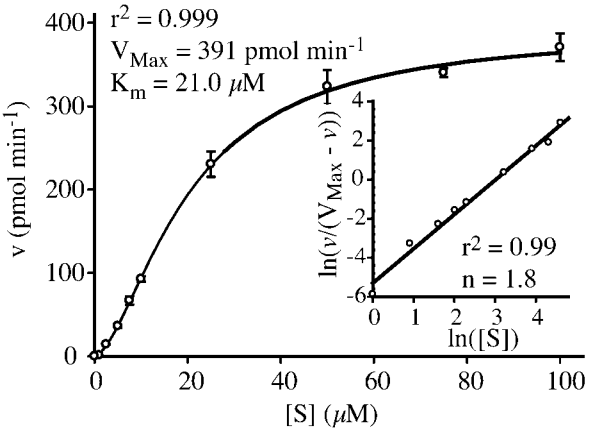

Fig. 3. The hydrolysis of *threo*-9/10-PHO by purified HsEH was analyzed by using the Hill equation as described in the text. Shown is the mean ± standard deviation of the reaction velocity (v) as a function of substrate concentration [S] of a representative experiment. (*Inset*) Hill plot documents the observed positive cooperativity in substrate hydrolysis.

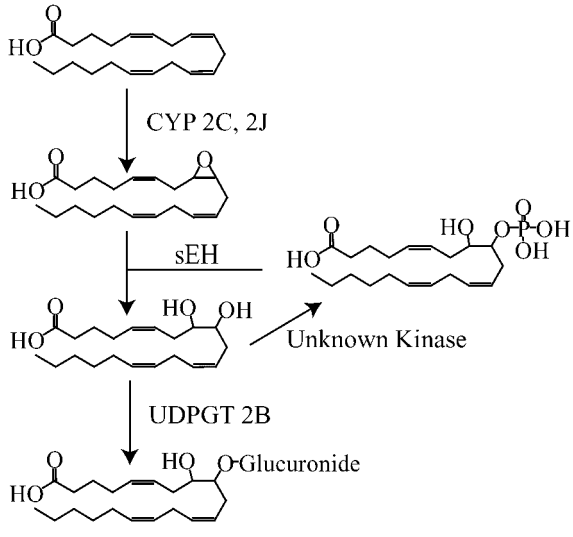

Fig. 4. The identification of dihydroxy lipid phosphates as high-affinity substrates for the sEH phosphatase domain suggests the existence of a novel branch to the polyunsaturated fatty acid metabolic cascade emanating from P450-dependent epoxidation. The physiological implications of this expanded pathway are as yet unknown.

efficiency of the two catalytic domains for oleate-derived metabolites, i.e., epoxy stearic acid; using $k_{cat}/K_m = 28\ s^{-1}/11\ \mu M = 2.56 \times 10^6\ M^{-1}\cdot s^{-1}$ (29) vs. *threo*-PHO and $k_{cat}/K_m = 0.35\ s^{-1}/21\ \mu M = 1.67 \times 10^4\ M^{-1}\cdot s^{-1}$, we find that the EH domain is at least ≈150 times more efficient than the phosphatase domain. The K_ms for these reactions are similar, suggesting similar substrate affinities. However, the sEH $^{EH}k_{cat}$ is much greater than the sEH $^{Phos}k_{cat}$, suggesting that epoxide transformation is more rapid than hydroxy phosphate hydrolysis under conditions where these two substrates appear at equal concentrations. Therefore, the sEH is functionally suited to regulate the generation of an intracellular pulse of dihydroxy lipid phosphate, or perhaps other lipophilic phosphates, in response to epoxide formation within a cell. Without further careful study, it is difficult to speculate the physiological implications of this proposed pathway. However, assuming that dihydroxy lipid phosphates are the endogenous substrates for the sEH phosphatase domain, it would be logical for this activity to be associated with the physiological effects of fatty acid epoxides. In particular, these compounds may be responsible for a portion of the reported fatty acid diol-dependent biology (11, 38, 39). Alternatively, these compounds may have unknown effects, possibly opposing the regulatory function of epoxy fatty acids in various cell types. Regardless, this functional description of the *EPXH2* gene product suggests that dihydroxy lipid phosphates may play a role as intracellular second messengers as seen for phospholipids in the sphingosine/ceramide (40–43) and polyisoprenylphosphate (44) signaling pathways. Thus we hypothesize that both the N- and C-terminal domains of the sEH produce the same dihydroxy fatty acid product; however, they do so from different substrates.

Funding for this research was provided by National Institute of Environmental Health Sciences Grant R37 ES02710, Superfund Basic Research Program Grant P42 ES04699, Center for Environmental Health Sciences Grant P30 ES05705, Center for Children's Environmental Health and Disease Prevention Grant P01 ES11269, and University of California Biotechnology Training Grant 2001-07.

1. Gill, S. S., Hammock, B. D., Yamamoto, I. & Casida, J. E. (1972) in *Insect Juvenile Hormones: Chemistry and Action*, eds. Menn, J. J. & Beroza, M. (Academic, New York), pp. 177–189.
2. Hammock, B. D., Storms, D. H. & Grant, D. F. (1997) in *Comprehensive Toxicology*, ed. Guengerich, F. P. (Pergamon, Oxford), Vol. 3, pp. 283–305.
3. Zheng, J., Plopper, C. G., Lakritz, J., Storms, D. H. & Hammock, B. D. (2001) *Am. J. Respir. Cell. Mol. Biol.* **25,** 434–438.
4. Yu, Z., Xu, F., Huse, L. M., Morisseau, C., Draper, A. J., Newman, J. W., Parker, C., Graham, L., Engler, M. M., Hammock, B. D., *et al*. (2000) *Circ. Res.* **87,** 992–998.
5. Chacos, N., Capdevila, J., Falck, J. R., Martin-Wixtrom, C., Gill, S. S., Hammock, B. D. & Estabrook, R. A. (1983) *Arch. Biochem. Biophys.* **233,** 639–648.
6. Capdevila, J. H. & Falck, J. R. (2001) *Biochem. Biophys. Res. Commun.* **285,** 571–576.
7. Roman, R. J. (2001) *Physiol. Rev.* **82,** 131–185.
8. Sun, J., Sui, X., Bradbury, J. A., Zeldin, D. C., Conte, M. S. & Liao, J. K. (2002) *Circ. Res.* **90,** 1020–1027.
9. Node, K., Huo, Y., Ruan, X., Yang, B., Spiecker, M., Ley, K., Zeldin, D. C. & Liao, J. K. (1999) *Science* **285,** 1276–1279.
10. Weintraub, N. L., Fang, X., Kaduce, T. L., VanRollins, M., Chatterjee, P. & Spector, A. A. (1999) *Am. J. Physiol.* **277,** H2098–H2108.
11. Greene, J. F., Williamson, K. C., Newman, J. W., Morisseau, C. & Hammock, B. D. (2000) *Arch. Biochem. Biophys.* **376,** 420–432.
12. Greene, J. F., Newman, J. W., Williamson, K. C. & Hammock, B. D. (2000) *Chem. Res. Toxicol.* **13,** 217–226.
13. Chen, J.-K., Capdevila, J. & Harris, R. C. (2002) *Proc. Natl. Acad. Sci. USA* **99,** 6029–6034.
14. Imig, J. D., Zhao, X., Capdevila, J. H., Morisseau, C. & Hammock, B. D. (2002) *Hypertension* **39,** 690–694.
15. Sinal, C. J., Miyata, M., Tohkin, M., Nagata, K., Bend, J. R. & Gonzalez, F. J. (2000) *J. Biol. Chem.* **275,** 40504–40510.
16. Beetham, J. K., Tian, T. & Hammock, B. D. (1993) *Arch. Biochem. Biophys.* **305,** 197–201.
17. Beetham, J. K., Grant, D., Arand, M., Garbarino, J., Kiyosue, T., Pinot, F., Oesch, F., Belknap, W. R., Shinozaki, K. & Hammock, B. D. (1995) *DNA Cell Biol.* **14,** 61–71.
18. Argiriadi, M. A., Morisseau, C., Hammock, B. D. & Christianson, D. W. (1999) *Proc. Natl. Acad. Sci. USA* **96,** 10637–10642.
19. Collet, J. F., Stroobant, V., Pirard, M., Delpierre, G. & Van Schaftingen, E. (1998) *J. Biol. Chem.* **273,** 14107–14112.
20. Collet, J. F., Stroobant, V. & Van Schaftingen, E. (1999) *J. Biol. Chem.* **274,** 33985–33990.
21. Ndubuisil, M. I., Kwok, B. H., Vervoort, J., Koh, B. D., Elofsson, M. & Crews, C. M. (2002) *Biochemistry* **41,** 7841–7848.
22. Enright, A. J., Iliopoulos, I., Kyrpides, N. C. & Ouzounis, C. A. (1999) *Nature* **402,** 86–90.
23. Marcotte, E. M., Pellegrini, M., Ng, H. L., Rice, D. W., Yeates, T. O. & Eisenberg, D. (1999) *Science* **285,** 751–753.
24. Newman, J. W. & Hammock, B. D. (2001) *J. Chromatogr. A* **925,** 223–240.
25. Wixtrom, R. N., Silva, M. H. & Hammock, B. D. (1988) *Anal. Biochem.* **169,** 71–80.
26. Yamada, T., Morisseau, C., Maxwell, J. E., Argiriadi, M. A., Christianson, D. W. & Hammock, B. D. (2000) *J. Biol. Chem.* **275,** 23082–23088.
27. Grant, D. F., Greene, J. F., Pinot, F., Borhan, B., Moghaddam, M. F., Hammock, B. D., McCutchen, B., Ohkawa, H., Luo, G. & Guenthner, T. M. (1996) *Biochem. Pharmacol.* **51,** 503–515.
28. Morisseau, C., Beetham, J. K., Pinot, F., Debernard, S., Newman, J. W. & Hammock, B. D. (2000) *Arch. Biochem. Biophys.* **378,** 321–332.
29. Borhan, B., Mebrahtu, T., Nazarian, S., Kurth, M. J. & Hammock, B. D. (1995) *Anal. Biochem.* **231,** 188–200.
30. Wixtrom, R. N. & Hammock, B. D. (1985) in *Biochemical Pharmacology and Toxicology*, eds. Zakim, D. & Vessey, D. A. (Wiley, New York), Vol. 1, pp. 1–93.
31. Ullman, B. & Perlman, R. L. (1975) *Biochem. Biophys. Res. Commun.* **63,** 424–430.
32. Segel, I. H. (1993) *Enzyme Kinetics: Behavior and Analysis of Rapid Equilibrium and Steady-State Enzyme Systems* (Wiley, New York).
33. Morisseau, C., Du, G., Newman, J. W. & Hammock, B. D. (1998) *Arch. Biochem. Biophys.* **356,** 214–228.
34. Morisseau, C., Goodrow, M. H., Dowdy, D., Zheng, J., Greene, J. F., Sanborn, J. R. & Hammock, B. D. (1999) *Proc. Natl. Acad. Sci. USA* **96,** 8849–8854.
35. Argiriadi, M. A., Morisseau, C., Goodrow, M. H., Dowdy, D. L., Hammock, B. D. & Christianson, D. W. (2000) *J. Biol. Chem.* **275,** 15265–15270.
36. Morisseau, C., Goodrow, M. H., Newman, J. W., Wheelock, C. E., Dowdy, D. L. & Hammock, B. D. (2002) *Biochem. Pharmacol.* **63,** 1599–1608.
37. Jain, M. K. (1982) *Handbook of Enzyme Inhibitors, 1965–1977* (Wiley, New York).
38. Sisemore, M. F., Zheng, J., Yang, J. C., Thompson, D. A., Plopper, C. G., Cortopassi, G. A. & Hammock, B. D. (2001) *Arch. Biochem. Biophys.* **392,** 32–37.
39. Moran, J. H., Mon, T., Hendrickson, T. L., Mitchell, L. A. & Grant, D. F. (2001) *Chem. Res. Toxicol.* **14,** 431–437.
40. Levade, T., Auge, N., Veldman, R. J., Cuvillier, O., Negre-Salvayre, A. & Salvayre, R. (2001) *Circ. Res.* **89,** 957–968.
41. Spiegel, S. & Kolesnick, R. (2002) *Leukemia* **16,** 1596–1602.
42. Ogawa, C., Kihara, A., Gokoh, M. & Igarashi, Y. (2002) *J. Biol. Chem.* **278,** 1268–1272.
43. Hla, T., Lee, M. J., Ancellin, N., Paik, J. H. & Kluk, M. J. (2001) *Science* **294,** 1875–1878.
44. Levy, B. D. & Serhan, C. N. (2000) *Biochem. Biophys. Res. Commun.* **275,** 739–745.